Pis'ma v ZhETF, vol. 90, iss. 7, pp. 552 – 556

Plasmonic and magnetic effects accompanying optical second-harmonic generation in Au/Co/Au nanodisks

T. V. Murzina[1)], *I. A. Kolmychek, A. A. Nikulin, E. A. Gan'shina, O. A. Aktsipetrov*

Department of Physics, Moscow State University, 119992 Moscow, Russia

Submitted 31 July 2009

Optical second-harmonic (SH) generation in Au/Co/Au sandwich-like nanodisks is studied, using several experimental techniques, at SH frequency being close to that of the plasmon resonance in the system. The dependences of the relative amplitude and phase of the magnetization-induced SH component on the angle of incidence are found to significantly differ from those measured for a continuous Au/Co/Au trilayer film. A phenomenological description of the observed effects is proposed, with special emphasis on resonant excitation of the local plasmon modes by the nonlinear sources induced in the nanodisks.

PACS: 42.65.–k, 75.50.–y

Light can be strongly affected by resonant coupling to local plasmon modes in metallic nanosructures [1]. The idea to manipulate light on the nanoscale by means of local-plasmon excitation has given rise to numerous experimental and theoretical studies that found a new field of research, plasmonics. The nonlinear-optical aspect of these studies is of particular interest, because the efficiency of Raman scattering or second- and third-harmonic generation from nanostructured plasmonic systems like rough metal surfaces [2] or arrays of metallic nanoparticles [3, 4] increases by several orders of magnitude due to the local-plasmon resonances. Another topical aspect is magneto-optics of nanostructures combining magnetic and plasmonic features. Typically, these are composite nanostructures comprised of plasmonic and magnetic constituents, e.g., heterostructures with adjacent layers of a noble metal and a ferromagnetic [5, 6] (plasmons in magnetic metals proper are overdamped because of large absorption). Large enhancement of the magneto-optical Faraday and Kerr effects in bilayer plasmonic/magnetic structures is predicted in [7]. Experimental observations of plasmon-enhanced magneto-optical effects are reported in [5] for Au/Co/Au sandwich-like nanodisks and in [8, 9] for continuous Au/Co/Au trilayer films.

To date, researchers' attention has been focused on linear-optical effects in plasmonic/magnetic systems. In this letter the magnetization-induced second-harmonic generation (SHG) from Au/Co/Au nanodisks in the spectral vicinity to the local-plasmon resonance is studied with combining three experimental techniques based on measuring (a) the SH scattering indicatrices and wave-polarization patterns, (b) SHG magnetic contrast, and (c) magnetization-induced phase shift of the SH signal. To detect morphology-specific features in the measured data the latter are compared with those for a continuous Au/Co/Au film treated as a reference system.

Continuous Au/Co/Au films were deposited on a glass substrate by magnetron sputtering, with the layers being 6, 10 and 16 nm thick, respectively. Sandwich-like nanodisks were fabricated from the continuous films by colloidal lithography, using polystyrene spheres of 110 nm in diameter as described in [5]. According to the AFM analysis, the nanodisks are randomly distributed on the substrate with the filling factor of about 0.2. The in-plane magnetization of the nanodisks saturates in the DC magnetic field of about 1 kOe.

Figure 1a shows the absorption spectrum of the nanodisks. The spectrum exhibits a plasmon peak at 2 eV with the half-width of about 0.5 eV. The contrast δ_ω of the magneto-optical Kerr effect (MOKE) defined as $\delta_\omega = \left(I_\omega^M - I_\omega\right)/I_\omega$, where I_ω^M (I_ω) is the value of the linearly-reflected light intensity in the presence (absence) of the DC magnetic field, was measured in the transversal geometry [10] at room temperature and angle of incidence of 65°, with applying the DC magnetic field of 3 kOe. According to Fig.1b, a double-minimum feature occurs in the spectrum of δ_ω for nanodisks, contrary to that for the reference trilayer.

For the nonlinear-optical experiments the p-polarized output of a YAG: Nd^{3+} laser at 1064 nm wavelength was used, with pulse duration of 15 ns and pulse intensity of 1 MW/cm^2. Noteworthily, the SH wavelength value of 532 nm (which corresponds to the photon energy of 2.34 eV) falls within the half width of the plasmon-peak shown in Fig.1a. The SH radiation from the studied samples was spectrally selected with an appropriate set

[1)] e-mail: mur@shg.ru

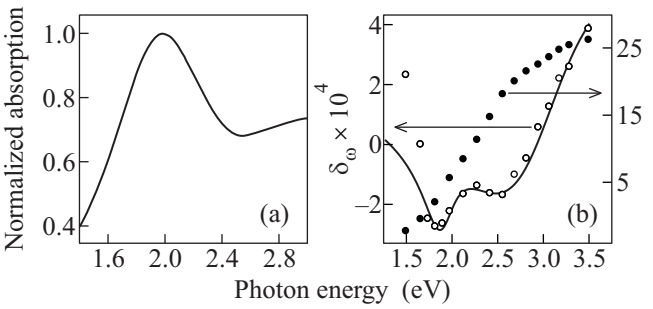

Fig.1. Panel (a), absorption spectrum measured for nanodisks. Panel (b), MOKE contrast spectra measured for nanodisks (open circles) and trilayer film (solid circles). Solid line in panel (b), approximation of the experimental data with Eq. (9) for nanodisks at $\hbar\Omega_N = \hbar\Omega_M = 1.90$ eV, $\Gamma_N = 0.43\Omega_N$, $\Gamma_M = 0.11\Omega_N$, $B = 9.59 \cdot 10^{-4} \cdot (1 - i)$, $C_N = -0.99$, $C_M = 2.57 \cdot 10^{-4}$

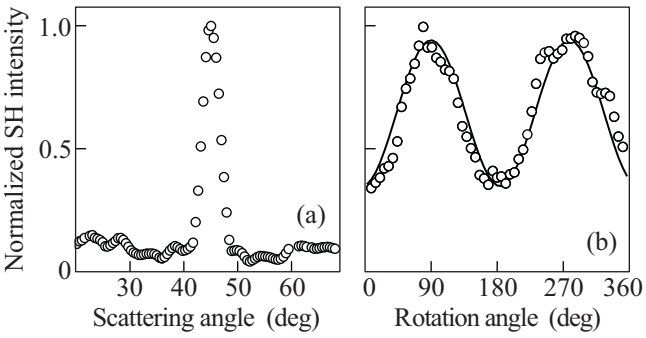

Fig.2. Panels (a) and (b), SHG indicatrix and wave-polarization patterns, respectively. Open circles, experimental data for nanodisks; solid line in panel (b), approximation of the data by the dependence $\eta + \zeta\cos(2\phi + \phi_0)$, where ϕ is the analyzer rotation angle, η, ζ and ϕ_0 are adjustable parameters. The scattering angle is counted from the normal to the sample, the analyzer rotation angles 90° and 270° correspond to p-polarization

of filters and detected by a PMT and gated electronics. The magnetization-induced effects were studied in the geometry of the transversal nonlinear magneto-optical Kerr effect, with applying the DC magnetic field of 2 kOe in either direction. The dependence of the SH intensity on the angle of incidence was measured in the specular direction for the p-polarized SH component. The relative phase of the SH signal was measured using the SH interferometry scheme described in [11] with a thin ITO film in the role of the SH signal reference.

To estimate the strength of hyper-Rayleigh scattering (HRS), i.e. the generation of incoherent (diffuse and depolarized) SH radiaion due to the in-plane disorder of the nanodisks array, the SH scattering indicatrices and wave-polarization patterns were measured at the angle of incidence fixed at 45° (Fig.2). HRS reveals itself in nonzero values of the SH intensity detected in off-specular directions in the scattering indicatrix and in the minima of the wave-polarization pattern. At the same time, as it can be seen from Fig.2, the SH radiation contains a significant coherent (specular and p-polarized) component.

In order to represent the obtained nonlinear magneto-optical data with emphasis on the magnetization-induced changes, an appropriate set of quantities should be introduced. The measured ones are the intensities $I^+_{2\omega}$, $I^-_{2\omega}$ and phases $\varphi^+_{2\omega}$, $\varphi^-_{2\omega}$ corresponding to opposite directions of the DC magnetic field. The intensities $I^+_{2\omega}$ and $I^-_{2\omega}$ can be expressed through the superposition of two fields:

$$I^{\pm}_{2\omega} \propto \left|E^N_{2\omega} \pm E^M_{2\omega}\right|^2, \qquad (1)$$

where $E^N_{2\omega}$ is the complex amplitude of the p-polarized component of the SH electric field originating from the non-magnetic (crystallographic) SH sources and $E^M_{2\omega}$ is the complex amplitudes pertaining to the p-polarized component of the field generated by the magnetization-induced SH sources. The dominating contribution to $E^M_{2\omega}$ is given by the term linear in the magnetization, whence the change of sign in Eq. (1) stems. Therefore, the magnetization-induced SH component can be characterized by introducing the amplitude factor $\gamma_{2\omega} = \left|E^M_{2\omega}\right| / \left|E^N_{2\omega}\right|$ and the relative phase shift $\Phi_{2\omega} = \arg\left(E^M_{2\omega}/E^N_{2\omega}\right)$. These quantities are related to $I^{\pm}_{2\omega}$ and $\varphi^{\pm}_{2\omega}$ as the follows:

$$\gamma_{2\omega} = \frac{F_-}{F_+}, \quad \Phi_{2\omega} = \arccos\left(\frac{\rho_{2\omega}F_+}{2F_-}\right), \qquad (2)$$

where

$$F_\pm = \left[1 \pm \left(1 - \rho^2_{2\omega}\right)^{1/2}\cos\varphi_{2\omega}\right]^{1/2},$$

$$\rho_{2\omega} = \frac{I^+_{2\omega} - I^-_{2\omega}}{I^+_{2\omega} + I^-_{2\omega}}, \quad \varphi_{2\omega} = \varphi^+_{2\omega} - \varphi^-_{2\omega}.$$

Similarly, the MOKE contrast δ_ω can be represented in the form: $\delta_\omega = 4\mathrm{Re}\left(E^M_\omega/E^N_\omega\right)$, where E^N_ω and E^M_ω are the linear-optical analogs of the complex amplitudes $E^N_{2\omega}$ and $E^M_{2\omega}$, respectively.

The experimental dependences of the amplitude factor $\gamma_{2\omega}$ and relative phase shift $\Phi_{2\omega}$ on the angle of incidence of the fundamental beam are shown in Fig.3. One can see that for nanodisks they significantly differ from those for the reference trilayer.

The obtained results can be interpreted as follows.

(i) The linear-absorption peak shown in Fig.1a is observed at normal incidence, which indicates that local surface plasmons in nanodisks are resonantly excited by the electric-field component lying in the plane

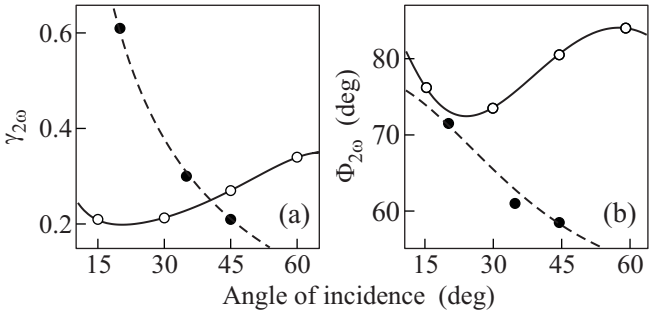

Fig.3. Panels (a) and (b), amplitude factor $\gamma_{2\omega}$ and phase $\Phi_{2\omega}$, respectively, measured as functions of the angle of incidence for nanodisks (open sircles) and trilayer film (solid circles). The angle of incidence is counted from the normal to the sample. Solid and dashed lines, approximations of the experimental data with expressions given by Eqs. (15), (16) at the following values of the nonzero components of tensors $X^{\hat{\sigma},\tau}$: $X^{M,d}_{xxx} = (0.08+0.03i)X^{N,d}_{zzz}$, $X^{M,d}_{xzz}+X^{M,d}_{zzx} = (0.21+1.50i)X^{N,d}_{zzz}$, $X^{M,d}_{xxz}+X^{M,d}_{zxx} = (0.48-1.52i)X^{N,d}_{zzz}$, $X^{N,d}_{xxz} + X^{N,d}_{zxx} = (1.05 - 1.99i)X^{N,d}_{zzz}$ for nanodisks and $X^{M,f}_{xxx} = (0.07 + 0.06i)X^{N,f}_{zzz}$, $X^{M,f}_{xzz} + X^{M,f}_{zzx} = (0.12 + 0.15i)X^{N,f}_{zzz}$, $X^{N,f}_{xxz} + X^{N,f}_{zxx} = (0.33 - 0.25i)X^{N,f}_{zzz}$ for trilayer. The components are written out for the Cartesian frame in which the z-axis is normal to the plane of the sample and the x-axis is parallel to the plane of incidence

of the structure. This agrees with the estimations made for the Mie resonance in a homogeneous oblate spheroid [12] placed (in vacuum) in a uniform electric field perpendicular to the spheroid's axis of symmetry. In fact, for a spheroid with the same ratio of semiaxis lengths as the average diameter-to-height ratio for the studied nanodisks, the corresponding Mie resonance is attained at the real part of the dielectric constant of the spheroid material being about -5.5, which is close to the value for gold at 532 nm. It is worth to note that the geometry of both linear-optical and SHG measurements carried out excludes the possibility of resonant excitation of traveling plasmon-polaritons in the reference trilayer structure.

(ii) The two-minima feature in the MOKE contrast spectrum for nanodisks can be interpreted as also due to resonant plasmon excitation. To proceed with this explanation we treat each nanodisk in the array as a point dipole induced by incident monochromatic plane wave with frequency ω and wavevector $\mathbf{K}$. The total dipole moment of a single particle is $\mathbf{D}_\omega = \mathbf{D}^N_\omega + \mathbf{D}^M_\omega$, where $\mathbf{D}^N_\omega$ and $\mathbf{D}^M_\omega$ are the nonmagnetic and magnetization-dependent components, respectively. Being insignificant in the spectral range of interest, linear reflection from the glass substrate is neglected for simplicity in further considerations. Then the effective electric field $\mathbf{E}^{\rm eff}_\omega$ acting on a given nanodisk is the superposition of the field in the incident wave $\mathbf{E}_\omega$ and the fields from remaining nanodisks in the array. Since the typical nanodisk dimensions are much smaller than the wavelength of the incident radiation and particles are not conglomerated into close-packed clusters, the field $\mathbf{E}^{\rm eff}_\omega$ can be treated as uniform. The field $\mathbf{E}^{\rm eff}_\omega$ can be related with $\mathbf{E}_\omega$ by means of the local-factor $\hat{L}_\omega$ (throughout the paper caps over quantities denote tensors): $\mathbf{E}^{\rm eff}_\omega = \hat{L}_\omega \cdot \mathbf{E}_\omega$. Of key importance is the fact that the dipole moments $\mathbf{D}^N_\omega$ and $\mathbf{D}^M_\omega$ are induced in two different ways: $\mathbf{D}^N_\omega$ stems directly from nanodisk polarizing by the field $\mathbf{E}^{\rm eff}_\omega$ and is magnetization-independent, whereas $\mathbf{D}^M_\omega$ appears as a response to the electric field from the magnetization-dependent part of the linear polarization induced by $\mathbf{E}^{\rm eff}_\omega$ within the Co layer and vanishes in the absence of the static magnetization. This can be taken into account by introducing the polarizabilities $\hat{\alpha}^{N,M}_\omega$:

$$\mathbf{D}^\sigma_\omega = \hat{\alpha}^\sigma_\omega \cdot \mathbf{E}_\omega, \quad \sigma = N, M, \tag{3}$$

with

$$\hat{\alpha}^N_\omega = \frac{1}{4\pi}\int\limits_V [\varepsilon_\omega(z) - 1]\,\hat{\Lambda}_\omega(\mathbf{R})d\mathbf{R}, \tag{4}$$

$$\hat{\alpha}^M_\omega = \frac{1}{4\pi}\int\limits_V\int\limits_V \hat{F}^d_\omega(\mathbf{R},\mathbf{R}')\cdot\hat{\varepsilon}^M_\omega(z')\cdot\hat{\Lambda}_\omega(\mathbf{R}')d\mathbf{R}'d\mathbf{R}, \tag{5}$$

$$\hat{\Lambda}_\omega(\mathbf{R}) = \lim_{\xi\to\infty}\left[\hat{G}^d_\omega(\mathbf{R},\mathbf{R}+\xi\mathbf{x})\cdot\hat{Q}(\mathbf{x})\right]\cdot\hat{L}_\omega, \tag{6}$$

$$\hat{F}^d_\omega(\mathbf{R},\mathbf{R}') = \hat{L}_\omega\cdot\left[\hat{I}\delta(\mathbf{R}-\mathbf{R}') + \frac{\varepsilon_\omega(z)-1}{4\pi}\hat{G}^d_\omega(\mathbf{R},\mathbf{R}')\right], \tag{7}$$

where integration is carried out over the volume occupied by the nanodisk, $\hat{Q}(\mathbf{x}) = \frac{3}{2}\mathbf{x}\mathbf{x} - \hat{I}$, $\mathbf{x}$ is an arbitrary unit vector, $\hat{I}$ is the unit tensor, $\mathbf{R} = \{x, y, z\}$ is the three-dimensional radius-vector, the z-axis is directed along the nanodisk symmetry axis (i.e. perpendicular to the array plane), $\varepsilon_\omega(z)$ and $\hat{\varepsilon}^M_\omega(z)$ are piecewise-constant functions describing the spatial distribution of the dielectric permittivity inside the nanodisk, i.e. $\varepsilon_\omega(z) = \varepsilon^{\rm Au}_\omega$ within two regions occupied by Au: $z_1 < z < z_2$ and $z_2 + \Delta_{\rm Co} < z < z_1 + \Delta$, $\varepsilon_\omega(z) = \varepsilon^{\rm Co}_\omega$ within the Co layer: $z_2 < z < z_2 + \Delta_{\rm Co}$, $\hat{\varepsilon}^M_\omega(\mathbf{r}) = \hat{\varepsilon}^M_\omega$ within the Co layer, otherwise $\hat{\varepsilon}^M_\omega(\mathbf{r}) \equiv 0$, scalars $\varepsilon^{\rm Au}_\omega$ and $\varepsilon^{\rm Co}_\omega$ are the (nonmagnetic) complex dielectric constants of Au and Co, respectively, whereas $\hat{\varepsilon}^M_\omega$ is the magnetic part of the dielectric permittivity tensor of Co, Δ ($\Delta_{\rm Co}$) is the thickness of the nanodisk (Co layer), and $\hat{G}^d_\omega(\mathbf{r},\mathbf{r}')$ is the electromagnetic Green's function tensor for a single nanodisk in the electrostatic limit. The poles of $\hat{G}^d_\omega(\mathbf{r},\mathbf{r}')$ corresponding to plasmon modes of the nanodisks pro-

vide resonant behavior of the local-feid factor $\hat{\Lambda}_\omega$, tensor $\hat{F}^d_\omega$ and, hence, polarizabilities $\hat{\alpha}^{N,M}_\omega$.

Obviously,

$$E^\alpha_\omega \propto \mathbf{e}_p \cdot \langle \mathbf{D}^\sigma_\omega \rangle, \quad \sigma = N, M, \tag{8}$$

where $\mathbf{e}_p$ is the p-polarization ort in the plane wave propagating in the specular direction. Angular brackets denote statistical averaging over fluctuations of all parameters affecting the response of a nanodisk in the array, e.g., the particle shape and size, relative positions of neighboring particles, etc. Fluctuations lead to inhomogeneous resonance broadening. The latter evidently differs for $\langle \mathbf{D}^N_\omega \rangle$ and $\langle \mathbf{D}^M_\omega \rangle$, since the resonant quantity, $\hat{G}^d_\omega(\mathbf{r}, \mathbf{r}')$, enters into the effective polarizabilities $\hat{\alpha}^N_\omega$ and $\hat{\alpha}^M_\omega$ in different ways. In the vicinity of a single plasmon resonance this can be taken into account phenomenologically, by approximating the frequency dependence of $\langle \mathbf{D}^N_\omega \rangle$ and $\langle \mathbf{D}^M_\omega \rangle$ with two different Lorentzian contours (the Lorentzian spectral shape for both averaged quantities is chosen for simplicity). Thus from Eq. (8) we obtain the following expression for the MOKE contrast spectrum:

$$\delta_\omega = 4\mathrm{Re}\left[\frac{B + C_M(\omega - \Omega_M + i\Gamma_M)^{-1}}{1 + C_N(\omega - \Omega_N + i\Gamma_N)^{-1}}\right], \tag{9}$$

where B and $C_{N,M}$ are complex constants, $\Omega_{N,M}$ and $\Gamma_{N,M}$ are real positive ones, all treated as phenomenological parameters. It can be seen from Fig.1b that the dependence given by Eq. (9) reproduces the double-minimum feature in the MOKE contrast spectrum at the values of $\Omega_{N,M}$ and $\Gamma_{N,M}$ that are in reasonable agreement with the parameters of the measured absorption peak shown in Fig.1a.

(iii) According to the data on HRS (Fig.2), a small incoherent SH component can be neglected upon analyzing the dependences shown in Fig.3. For both nanodisk array and reference trilayer it is convenient to characterize the sources of the SH signal with the effective surface polarization (the dipole moment per unit area) $\Pi^{\sigma,\tau}_{2\omega}(\mathbf{r}) = \Pi^{\sigma,\tau}_{2\omega} e^{2i\mathbf{k}\cdot\mathbf{r}}$, where $\mathbf{r} = \{x, y\}$ is the radius-vector in the array (trilayer) plane, $\mathbf{k}$ is the component of $\mathbf{K}$ parallel to this plane, $\sigma = N, M$ and $\tau = d, f$, with N and M standing for the nonmagnetic and magnetization-dependent contributions, respectively, d and f denoting quantities that pertain to the nanodisks and trilayer film, respectively. The SH sources $\Pi^{\sigma,\tau}_{2\omega}$ comprise the nonlinear (quadratic) polarization proper, and the linear one induced at SH frequency by the field from the quadratic polarization. This is taken into account in the following expressions:

$$\Pi^{\sigma,\tau}_{2\omega} = \hat{X}^{\sigma,\tau} \vdots \mathbf{E}_\omega \mathbf{E}_\omega, \tag{10}$$

where

$$\hat{X}^{\sigma,d} = \nu \left\langle \int_V \int_V \hat{F}^d_{2\omega}(\mathbf{R}, \mathbf{R}') \cdot \hat{\chi}^{\sigma,d}(\mathbf{R}') d\mathbf{R}' d\mathbf{R} \right\rangle, \tag{11}$$

$$\hat{X}^{\sigma,f} = \int_{z_1}^{z_1+\Delta} \int_{z_1}^{z_1+\Delta} \hat{F}^f_{2\omega}(z, z') \cdot \hat{\chi}^{\sigma,f}_{2\omega}(z') dz' dz, \tag{12}$$

$$\hat{F}^f_{2\omega}(z, z') = \hat{I}\delta(z - z') + \frac{\varepsilon_{2\omega}(z) - 1}{4\pi} \hat{G}^f_{2\omega}(\mathbf{k}; z, z'), \tag{13}$$

ν is the surface concentration of nanodisks in the array, $\hat{\chi}^{\sigma,\tau}$ is the tensor of the quadratic susceptibility, the function $\hat{F}^d_{2\omega}(\mathbf{R}, \mathbf{R}')$ is given by Eq. (7) (with replacing ω by 2ω), $\hat{G}^f_{2\omega}(\mathbf{k}; z, z') = \int \hat{G}^f_{2\omega}(\mathbf{r}; z, z') e^{-i\mathbf{k}\cdot\mathbf{r}} d\mathbf{r}$, tensor $\hat{G}^f_{2\omega}(\mathbf{r} - \mathbf{r}'; z, z')$ is the electromagnetic Green's function of the trilayer film in vacuum (as in the case of nanodisks, linear reflection from the substrate is neglected for simplicity). The quadratic response of a composite system made of centrocymmetric materials has two distinct constituents, namely, of dipole and quadrupole origin: the former gives rise to the nonlinear polarization localized at the interfaces, whereas the latter reveals itself in the bulk. The susceptibility $\hat{\chi}^{\sigma,\tau}$ includes both dipole and quadrupole contributions, $\hat{\chi}^{\sigma,d}$ containing additional, as compared to $\hat{\chi}^{\sigma,f}$, dipole terms that correspond to the quadratic response of the lateral (parallel to the z-axis) surface bounding the nanodisk. Obviously, $\hat{\chi}^{M,\tau} \equiv 0$ outside the Co layer. Explicit expressions for the nonzero components of four tensors $\hat{\chi}^{\sigma,\tau}$ ($\sigma = N, M$, $\tau = d, f$) are omitted for brevity. It should be emphasized that tensors $\hat{\chi}^{\sigma,\tau}$ describe the system's nonlinear response to the external field $\mathbf{E}_\omega$, not to the local one, i.e. the local-field factors at the fundamental frequency have been already incorporated in $\hat{\chi}^{\sigma,\tau}$. At given external field $\mathbf{E}_\omega$, the local fields inside a metal nanodisk substantially differ, by relative amplitudes and phases of their components, from those inside a metal trilayer film. This results in an even more pronounced difference between the components of $\hat{\chi}^{\sigma,d}$ and $\hat{\chi}^{\sigma,f}$, because of their quadratic dependence on the local-field factors at frequency ω. Another physical distinction between the nanosisk array and trilayer film (with respect to SHG) stems from the difference in their linear response at 2ω, more specifically, in the explicit expressions for tensors $\hat{F}^d_{2\omega}$ and $\hat{F}^f_{2\omega}$. In particular, $\hat{F}^d_{2\omega}$ possesses a resonant term accounting for the excitation of the local plasmon modes of nanodisks by the nonlinear polarization.

By analogy with Eq. (8), we relate the complex field amplitudes $E^\sigma_{2\omega}$ with the SH sources $\Pi^{\sigma,\tau}_{2\omega}$:

$$E^\sigma_{2\omega} \propto \mathbf{e}_p \cdot \Pi^{\sigma,\tau}_{2\omega}, \quad \sigma = N, M, \quad \tau = d, f. \tag{14}$$

The dependence of the amplitude factor $\gamma_{2\omega}$ and the relative phase shift $\Phi_{2\omega}$ on the angle of incidence θ can be obtained from Eqs. (10)–(14) in the following form:

$$\gamma_{2\omega}(\theta) = |A_\tau(\theta)|, \quad \Phi_{2\omega}(\theta) = \arg A_\tau(\theta), \tag{15}$$

$$A_\tau(\theta) = \frac{\sum\limits_{j,l} A_{j,l}^{M,\tau} \sin^j\theta \cos^l\theta}{\sum\limits_{j,l} A_{j,l}^{N,\tau} \sin^j\theta \cos^l\theta}, \quad \tau = d, f. \tag{16}$$

where each nonzero coefficient $A_{j,l}^{\sigma,\tau}$ is a sum of the corresponding nonzero components of tensor $\hat{X}^{\sigma,\tau}$; explicit expressions for $A_{j,l}^{\sigma,\tau}$ are omitted for brevity.

According to Fig.3, the qualitative difference between the dependences measured for the nanodisk array and trilayer film can be reproduced by Eqs. (15), (16). Although the adjusted values of the components of $\hat{X}^{\sigma,\tau}$ can be verified neither experimentally nor by ab initio calculations, the very numerical difference between these quantities for the nanodisk array and trilayer film has clear physical nature discussed above.

To conclude, applying the optical field $\mathbf{E}_\omega$ in the presence of the static magnetization $\mathbf{M}$ induces in a system different nonlinear polarizations (in this particular work we deal with those propotional to $\mathbf{ME}_\omega$, $\mathbf{E}_\omega\mathbf{E}_\omega$, and $\mathbf{ME}_\omega\mathbf{E}_\omega$). Each of them provides its own specific way to excite plasmon modes "from the inside", as opposed to the direct plasmon excitation "from the outside", i.e. by the external field $\mathbf{E}_\omega$. As a result, the choice of the relative magnitudes E_ω^M/E_ω^N and $E_{2\omega}^M/E_{2\omega}^N$ as basic quantities under study has proved to be an indicative way to characterize the interplay between magneto-optical and plasmonic effects on the nanoscale level.

The authors thank G. Armelles and A. Cebollada (Instituto de Microelectronica de Madrid) for composition of the samples and measurement of the absorption spectrum. This work is supported by the RFBR Grants #07-02-01358 and #08-02-01020, and the Presidential Grant for Leading Russian Science Schools НШ-1619.2008.2.

1. D. W. Berreman, Phys. Rev. **163**, 855 (1967).
2. C. K. Chen, A. R. B. de Castro, and Y. R. Shen, Phys. Rev. Lett. **46**, 145 (1981).
3. A. Wokaun, J. G. Bergman, J. P. Heritage et al., Phys. Rev. B **24**, 849 (1981).
4. E. M. Kim, S. S. Elovikov, T. V. Murzina et al., Phys. Rev. Lett. **95**, 227402 (2005).
5. J. B. Gonzalez-Diaz, A. Garcia-Martin, J. M. Garcia-Martin et al., Small **4**, 202 (2008).
6. P. Gangopadhyay, S. Gallet, E. Franz et al., IEEE Transactions on Magnetics **41**, 10, 4194 (2005).
7. V. I. Belotelov, L. L. Doskolovich, and A. K. Zvezdin, Phys. Rev. Lett. **98**, 077401 (2007).
8. C. Hermann, V. A. Kosobukin, G. Lampel et al., Phys. Rev. B **64**, 235422 (2001).
9. J. J. B. Gonzalez-Diaz, A. Garcia-Martin, G. Armelles et al., Phys. Rev. B **76**, 153402 (2007).
10. E. Gan'shina, V. Guschin, I. Romanov, and A. Tselev, J. Magn. Magn. Mater. **185**, 258 (1998).
11. O. A. Aktsipetrov, T. V. Murzina, E. M. Kim et al., J. Opt. Soc. Am. B **22**, 138 (2005).
12. L. D. Landau and E. M. Lifshitz, *Electrodynamics of Continuous Media*, Pergamon, New York, 1986.